



# Factors that influence the chemical composition and evolution of shallow groundwater in an arid region: a case study from the middle reaches of the Heihe River, China

Zongjun Gao<sup>1</sup> · Zhenyan Wang<sup>1</sup> · Shu Wang<sup>1</sup> · Xi Wu<sup>2</sup> · Yonghui An<sup>2</sup> · Wenxiang Wang<sup>3</sup> · Jiutan Liu<sup>1</sup>

Received: 4 May 2019 / Accepted: 28 June 2019 / Published online: 5 July 2019  
© Springer-Verlag GmbH Germany, part of Springer Nature 2019

## Abstract

To investigate the chemical characteristics, spatial distribution and evolution of groundwater in the middle reaches of the Heihe River, 100 shallow groundwater samples were collected and tested. The results of this assessment indicate that the shallow groundwater in the study area is weakly alkaline and brackish. Concentrations of  $K^+$ ,  $Cl^-$  and  $NO_3^-$  are highly variable in groundwater and are the highest in areas with intensive human land use activities. The TDS content of groundwater gradually increases from the recharge area to the discharge area, and the chemical composition gradually changes from  $SO_4^{2-}-HCO_3^- -Na^+ \cdot Mg^{2+}$  to  $SO_4^{2-} -Na^+ -Mg^{2+}$ . Overall, the chemical composition and groundwater types in the study area are primarily affected by water–rock reactions, and certain areas are more affected by human activities. Isotopic evidence indicates that the main source of shallow groundwater in the study area is snowmelt.

**Keywords** Arid regions · Shallow groundwater · Hydrochemical characteristics · Hydrogen oxygen isotope · Northwest China

## Introduction

Arid regions throughout the world commonly have a limited availability of water resources to aid regional development (Shen and Chen 2010). In many regions, there is insufficient information available to adequately manage water resources, particularly for managing groundwater use (Gleick 2000). In semiarid and arid regions, it is especially important to identify the factors that influence water quality and availability to enable effective and sustainable water resource management.

This is the situation on the Heihe River Basin, an arid region in the northwestern part of China. Located deep in the hinterland of the Eurasian continent, the middle reaches of the Heihe River are rich in natural resources, and the region

is strategically important. The region is also China's major western strategic deployment area. However, development in the region is currently restricted by the limited availability and poor quality of water (Yang 2006).

The Heihe River Basin is the second largest and most environmentally sensitive river basin in the northwest arid region of China. The basin is located in an arid and semi-arid climate area, with strong seasonal precipitation, strong surface evaporation and a highly fragile ecological environment (Lu et al. 2001a; Qi and Luo 2005). The discharge of the Heihe River varies seasonally, and the quaternary alluvial sediments that underlie the Heihe River Basin are 300–1200 m thick, which makes these sediments suitable for groundwater storage (Chen et al. 2014). The way in which to rationally use water resources to ensure their continued availability and quality to meet the needs of economic and social development has become a hot issue in the region.

Although there is a large body of international research on the factors that influence groundwater quality and availability in semiarid and arid regions, most of these studies are based on a limited number of samples (even in large study areas) due to the difficulties of carrying out groundwater investigations in these regions (Bouragba et al. 2011; Fantong et al. 2009). However, to guarantee the quality and

✉ Zongjun Gao  
zongjungao1964@163.com

<sup>1</sup> Shandong University of Science and Technology,  
Qingdao 266510, Shandong, China  
<sup>2</sup> Center for Hydrogeology and Environmental Geology  
Survey, Geological Survey China, Baoding 071051, Hebei,  
China  
<sup>3</sup> Weifang University, Weifang 261000, Shandong, China

quantity of groundwater, it is necessary to understand the hydrogeochemical characteristics of a groundwater flow system and the factors that have influenced its chemical composition. Consequently, many samples are usually required to confidently interpret the groundwater quality dataset.

The study of water resources in the Heihe River Basin began in the last century. In recent decades, the Chinese government and scientists from numerous disciplines have conducted several studies on water resources in the basin, including studies to assess water level changes, water quality and vegetation changes (Lu et al. 2001a; Ning et al. 2008). However, an insufficient amount of studies have been carried out in the middle reaches of the basin to provide baseline information for management purposes. For example, little research has been conducted on the factors that control the chemical composition of groundwater in this part of the basin or on the processes that influence groundwater recharge and discharge in this region. However, many groundwater samples have been collected in the region, and this information can aid in investigating the processes that influence groundwater hydrochemistry and the water cycle in other arid basins in similar geological settings worldwide.

To improve the ecological environment in the area, it is of substantial practical significance to determine the present groundwater situation in the Heihe River Basin, including the pattern of its movement and its chemical composition. In this study, groundwater quality data from 100 shallow groundwater samples in the middle reaches of the Heihe River were used to analyse the hydrochemical characteristics and spatial distribution of the shallow groundwater in the study area. In combination with regional hydrogeological information, we seek to elucidate: (1) the hydrochemical composition of the shallow groundwater in the middle reaches of the Heihe River Basin; (2) how the chemical composition of shallow groundwater changes with groundwater flow in the middle reaches of the basin; (3) the factors that influence hydrochemical composition along the groundwater flow in the middle reaches of the basin; and (4) the source of shallow groundwater recharge in the basin's middle reaches.

## Materials and method

### Physical characteristics of the study sites

The Heihe River Basin is the second-largest inland river basin in the arid and semiarid regions of northwest China (Lu et al. 2001b). The basin is also part of the Hexi Corridor working area in the key hydrogeological survey region of China. The study area is located in the Heihe River's middle reaches between 97°45' ~ 101°00'E and 38°23'40" ~ 40°30'00"N (Fig. 1), with a total area of approximately 11,100 km<sup>2</sup>.

The topography of the study area exhibits an NWW trend, with the river basin being sandwiched between two areas of significantly elevated topography. The topography is generally higher in the southern part of the region and decreases in elevation in the northerly direction. The southern part of the region has alpine characteristics that progressively become subalpine in nature in the westerly direction.

Due to the Heihe River Basin's location deep within the Eurasian hinterland and its great distance from the ocean, the basin is influenced by the atmospheric circulation of the Qinghai–Tibet Plateau and Mongolian desert. The region experiences a typical continental arid climate (climate type Bsk in the Köppen–Geiger classification system) with low humidity and strong winds. The average temperature in the region is 7.3 °C, the average annual rainfall is 130.4 mm, and the average evaporation is 2002.5 mm. The main stream of the Heihe River is the largest river in the basin, with a total length of 821–827 km. Together with 34 other independent surface rivers in the region, the river system of the Heihe River Basin is formed. Except for several small rivers originating in Dahuang Mountain, all other rivers originate in the Qilian Mountains area.

Groundwater in the region occurs in a number of different aquifer types, including fractured bedrock aquifers, porous-medium aquifers in sedimentary rocks, and porous-medium aquifers in unconsolidated sediments.

The most significant fractured-rock aquifers occur in the Qilian Mountains and the Longshou Shan and Heli Shan Mountains. Although these areas have a dry climate with limited precipitation and large evaporation rates, rocks in these areas are highly fissured due to faulting, jointing and the effects of weathering, which provide good conditions for groundwater occurrence. However, water quality in these aquifers is often poor due to the limited recharge rate from rainfall.

Groundwater in porous-medium sedimentary rock aquifers is distributed in the Qilian Mountains in the south and Longshou Shan and Heli Shan in the north. This type of groundwater is primarily supplied by meteoric water, and the recharge source is limited. Thus, the groundwater is generally poor quality.

Porous-medium aquifers in unconsolidated sediments are mainly distributed in plain areas, although small amounts of groundwater in such aquifers also occur in alluvial sediments in mountain valleys. The groundwater depth in the plain area is shallowest in the middle of the alluvial plain (generally less than 3 m), and the groundwater depth increases with proximity to the mountains on both sides of the plain but generally does not exceed 30 m in this area. In the southern Qilian Mountains, the depth to groundwater commonly exceeds 200 m, and in the Xinba area, the depth to groundwater may reach 500 m (Fig. 2).

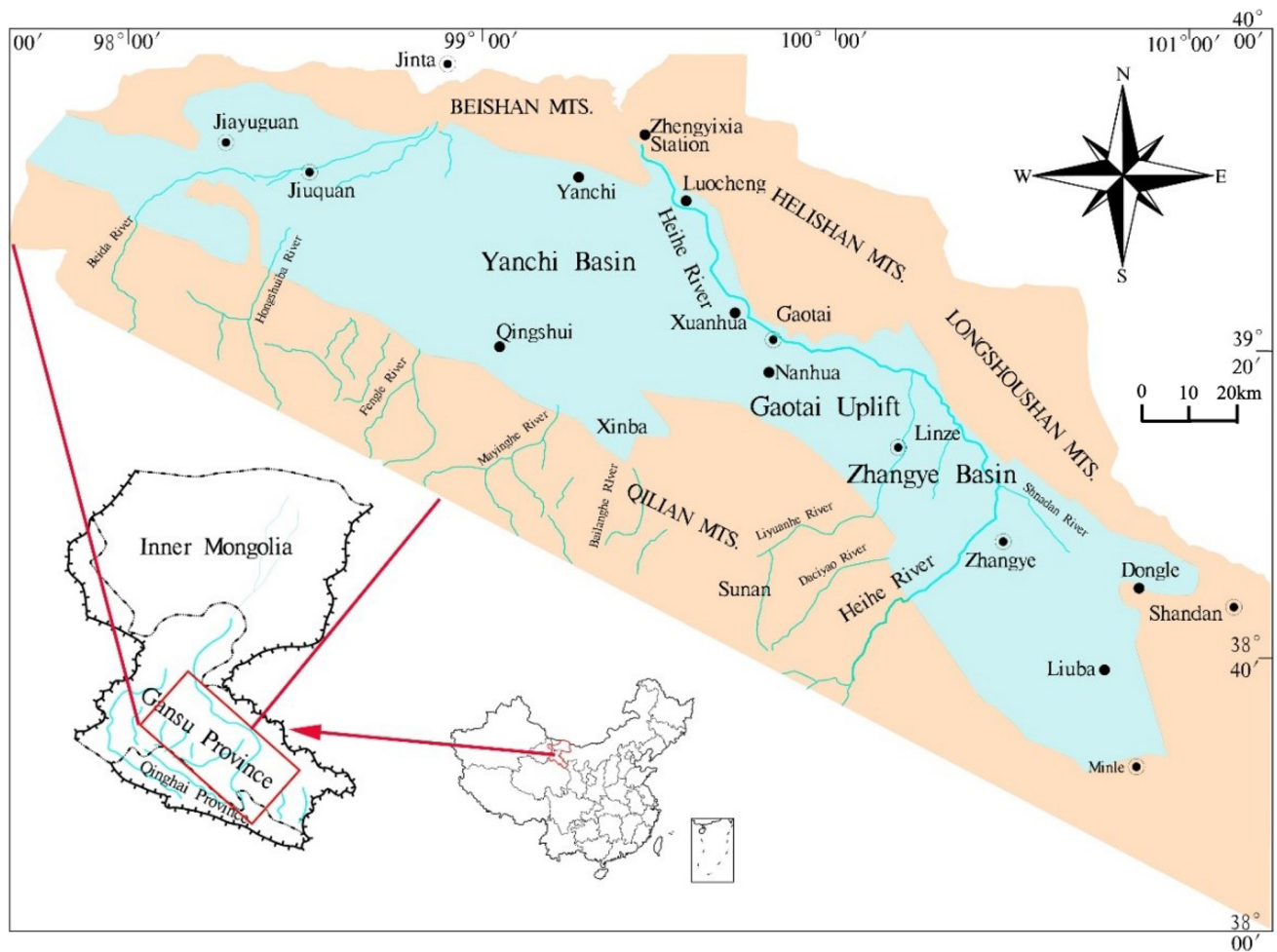


**Fig. 1** Study area location map. Light blue areas indicate basins, light brown areas indicate mountains

The groundwater flow direction in the study area is the same as the topographic trend but is restricted by the Gaotai uplift. Groundwater in the eastern part of the study area flows in the northwesterly direction, whereas groundwater in the western part of the study area flows in the northeasterly direction (Fig. 3).

## Sample collection and analytical methods

### Sample collection

A total of 100 shallow groundwater samples were collected in this study from July to August 2015. The samples that were collected included 15 samples from the Yanchi Basin, 61 samples from the Pediment, 16 samples from the Zhangye Basin, 3 samples from Heli Shan, 3 samples from the Qilian Mountains and 2 samples from the Gaotai uplift (Fig. 4). Water samples were taken from wells equipped with electric pumps, and the wells were not purged before samples were collected. The water samples were collected,

stored, and transported in strict accordance with the technical specifications for groundwater environmental monitoring (HJ/t164-2004).

The pH value and electrical conductivity of the groundwater samples were measured in the field using a multiparameter metre, and water levels were measured using a water level depth probe before water sampling was undertaken. The testing and analysis of other chemical constituents in the samples was performed in the Hydrogeological Survey Centre laboratory of the China Geological Survey.  $K^+$  and  $Na^+$  were determined by inductively coupled plasma atomic emission spectroscopy.  $Ca^{2+}$  and  $Mg^{2+}$  were determined by the EDTA titrimetric method.  $HCO_3^-$  was determined by titrimetry.  $SO_4^{2-}$  was determined by ethylenediamine tetraacetic acid disodium-barium titration.  $Cl^-$  was determined by argentometric titration.  $HNO_3^-$  was determined by ultraviolet spectrophotometry. Hydrogen and oxygen isotopes were detected by the TC/EA-IRMS method. The TDS was determined by the 180 °C oven drying method, and the pH was determined by the glass electrode method.

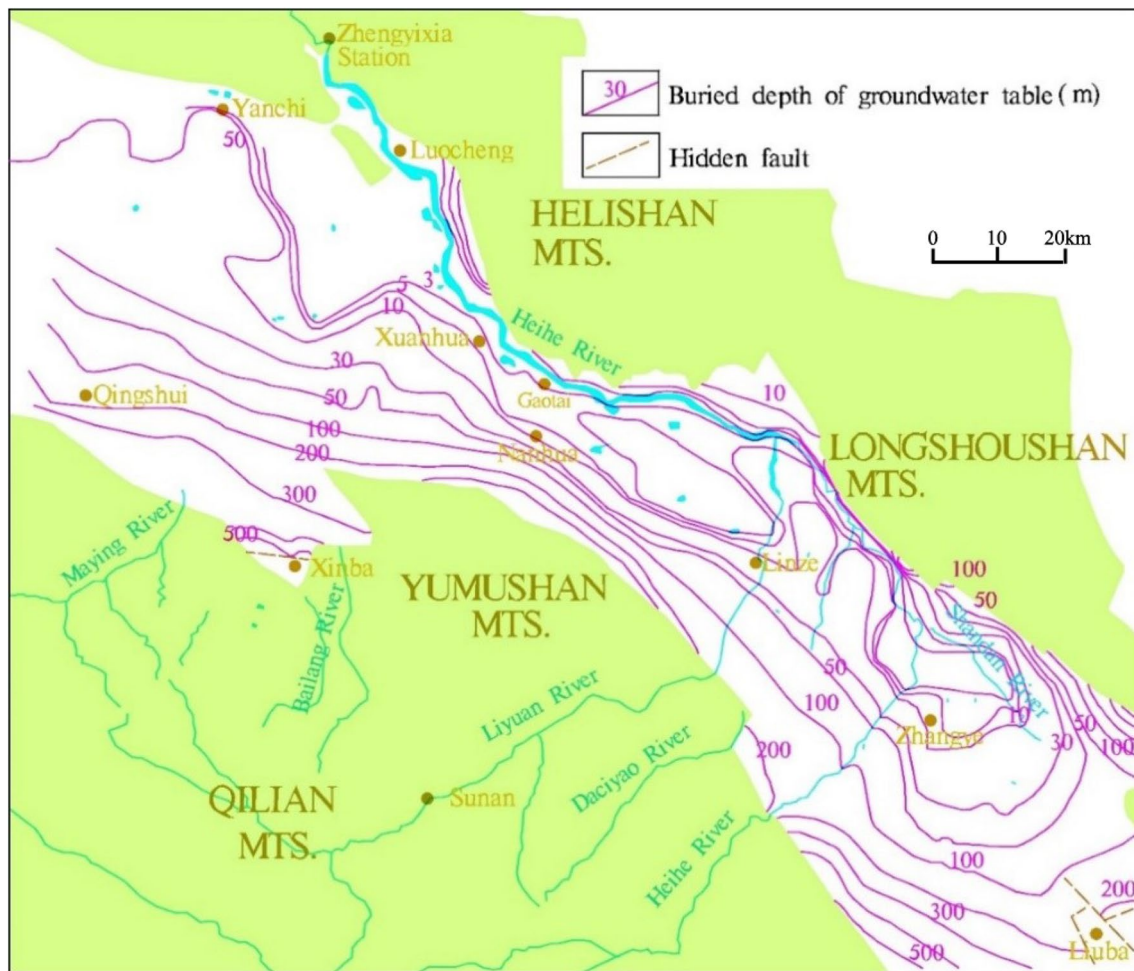


Fig. 2 Depth to groundwater contours for 2014

All operations were carried out in strict accordance with the China groundwater quality test method standard DZ/T 0064-1993 by the Ministry of Land and Resources, P. R. China.

## Data analysis methods

### Statistical analysis

Statistical parameters, including maximum values, minimum values, mean values, standard deviation, and coefficients of variation of the groundwater chemical data were calculated to determine the dominant ions, their order and stability.

Pearson correlation analyses were conducted to assess the correlations between various groundwater hydrochemical parameters. A correlation analysis of groundwater hydrochemical parameters can reflect their correlations and source differences by numerical values (Joshi and Seth 2011). In this analysis, IBM SPSS Statistics 19 software was used to calculate the Pearson correlation coefficient

between various hydrochemical parameters (Wang et al. 2007), and the correlation coefficient matrix of the hydrochemical parameters was obtained (Table 2).

Combined with recharge and discharge conditions, the change in the ion concentration in groundwater can reflect the progress of hydrochemical reactions in groundwater. Both of the previously mentioned statistical methods are used to describe the groundwater hydrochemical reaction process.

### Piper diagram

Major ion concentrations from groundwater samples collected in this study were plotted on a Piper diagram (Piper 1944) and used to analyse the composition of groundwater and infer the hydrochemical processes that have influenced water composition in the area.

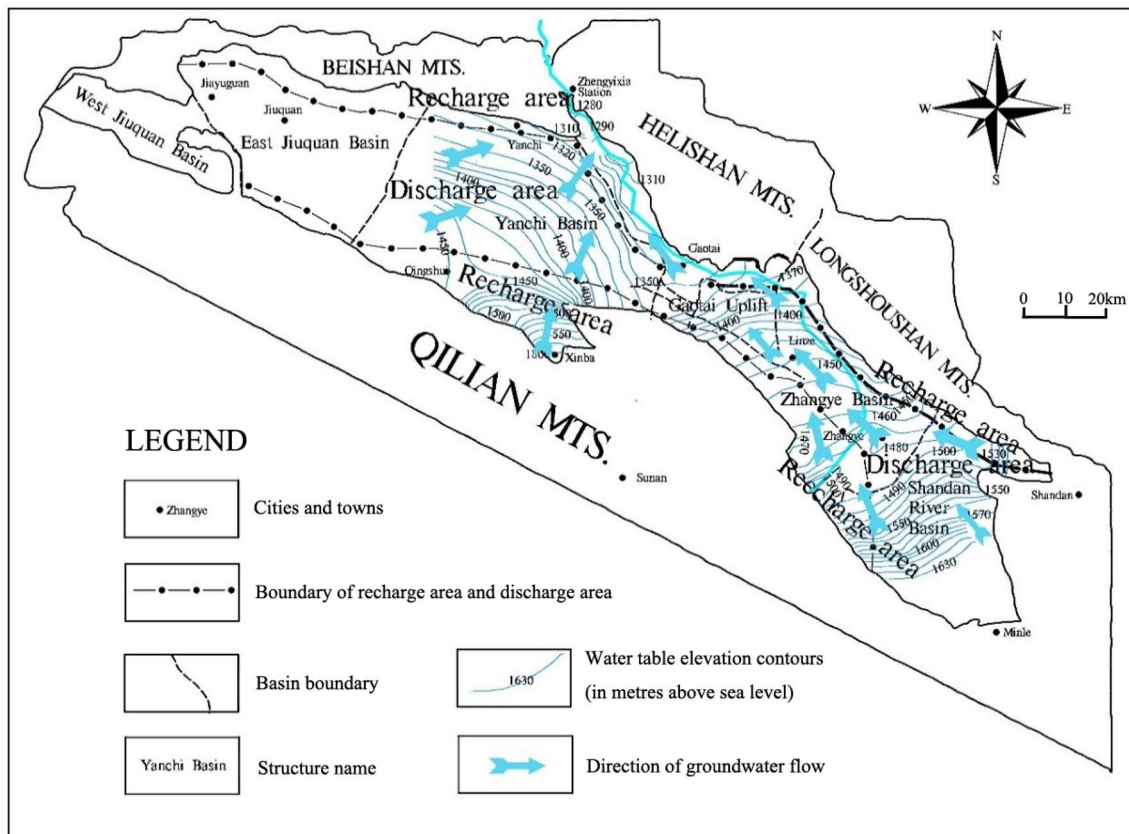


Fig. 3 Location of groundwater recharge and discharge areas and groundwater flow direction in the middle reaches of the Heihe River

**TDS contour map**

A contour map was compiled for TDS values of groundwater samples collected in this study. Due to the high density of sampling points in the Pediment, 16 points were selected at equal intervals as representative points for analysis and treatment together with sampling points in the Yanchi Basin, Zhangye Basin, Heli Shan, Qilian Mountain and the Gaotai uplift parts of the study area. The Piper diagram of the shallow groundwater in the research area was obtained using AqQA software (Fig. 5), and the TDS contour map of the research area was obtained using Surfer software (Fig. 6). The groundwater hydrochemical types were analysed according to the Shukarev classification (Dong et al. 2007).

**Gibbs plot**

The results of the chemical analyses were plotted on a Gibbs plot (Gibbs 1970) to identify the processes that are likely to have influenced the chemical composition of groundwater.

**Ion ratio graphs**

Groundwater quality data from samples in this study were plotted on ion ratio graphs to analyse the hydrochemical characteristics of the Heihe River middle reaches.

**Isotopes**

Measurements of stable isotope hydrogen and oxygen isotopes were used to determine the source of shallow groundwater (Craig 1961; Dansgaard 1964).

**Results and discussion**

**Hydrochemical characteristics of shallow groundwater**

Using the hydrochemical data obtained from the analysis of groundwater samples, the pH mass concentrations of TDS, Na<sup>+</sup>, K<sup>+</sup>, Ca<sup>2+</sup>, Mg<sup>2+</sup>, HCO<sub>3</sub><sup>-</sup>, Cl<sup>-</sup>, F<sup>-</sup>, NO<sub>3</sub><sup>-</sup>, SO<sub>4</sub><sup>2-</sup>, PO<sub>4</sub><sup>3-</sup> and Fe in the shallow groundwater samples were statistically analysed (Table 1). The findings are as follows. The

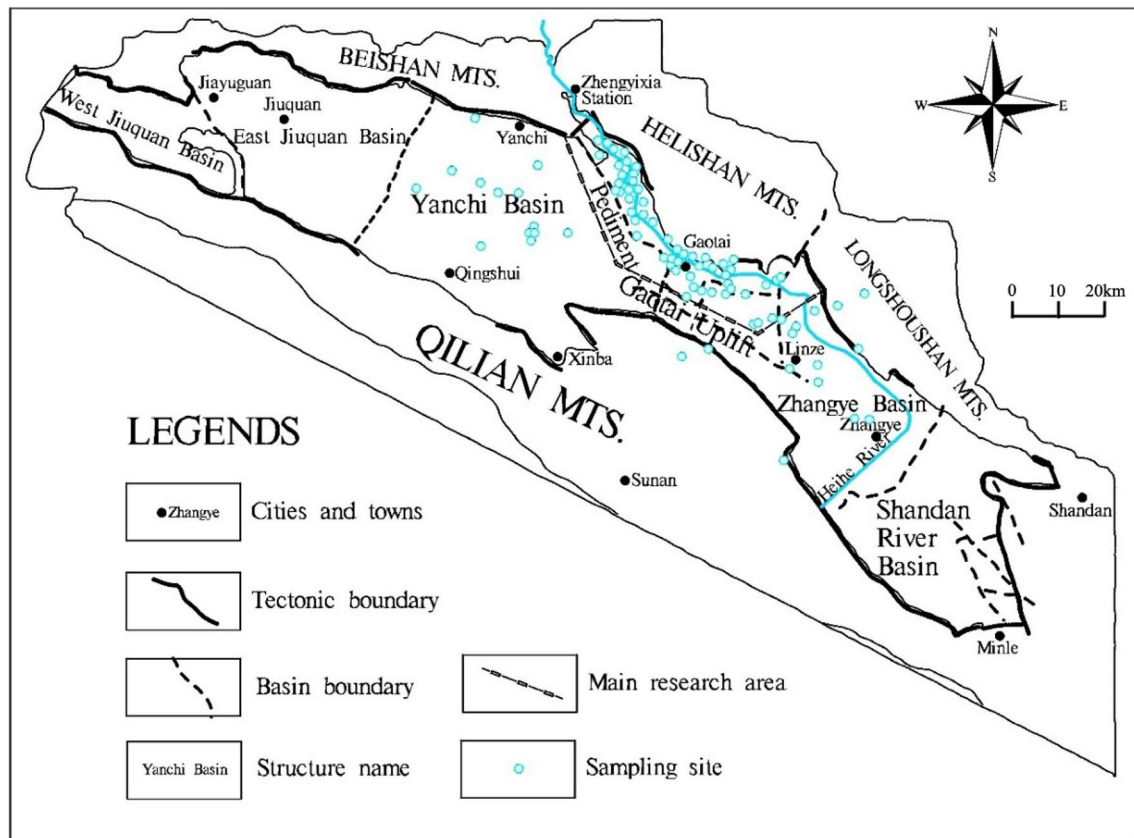


Fig. 4 Sampling site locations and distribution

pH value of the shallow groundwater varies between 7.26 and 9.72, with an average value of 7.87, which is weakly alkaline. The TDS of the shallow groundwater is between 205.3 and 4507 mg/L, with an average value of 1760 mg/L. That is, most shallow groundwater belongs to the brackish water category ( $1 \text{ g/L} < \text{TDS} < 3 \text{ g/L}$ ). Because most of the study area was in an arid basin, the occurrence of regional concentration results in an increase in TDS in the shallow groundwater. In addition, the influence of human activity in Gaotai and other cities and in all irrigated areas may also result in higher TDS values in the shallow groundwater.

The average concentrations of major cations in the groundwater in the study area were in the order of  $\text{Na}^+ > \text{Mg}^{2+} > \text{Ca}^{2+} > \text{K}^+$ , and the average anion concentration was in the order of  $\text{SO}_4^{2-} > \text{HCO}_3^- > \text{Cl}^- > \text{NO}_3^-$ . That is, the main anion in the study area is  $\text{SO}_4^{2-}$ , and the main cation is  $\text{Na}^+$ . This outcome corresponds to the hydrochemical characteristics of medium salinity water in this area.

In addition to the eight main ions, the  $\text{F}^-$ ,  $\text{PO}_4^{3-}$  and Fe concentrations were analysed. The results reveal that the average value of  $\text{F}^-$  in the study area was 0.48 mg/L, and the content was relatively low. These results suggest that the main source of  $\text{F}^-$  in groundwater was mineral

dissolution (Feng et al. 2004), and human made fluoride pollution was relatively light. The mean value of Fe was 0.08 mg/L, and the maximum value was only 0.29 mg/L, indicating that the iron content in the study area was low. The  $\text{PO}_4^{3-}$  content was slightly lower, with an average value of 0.03 mg/L and a maximum value of 0.06 mg/L.

The coefficient of variation can reflect the spatial differentiation to a certain extent (Huang and Zheng 2009; Liu 2012). The coefficients of variation (Cv) of  $\text{K}^+$ ,  $\text{Cl}^-$  and  $\text{NO}_3^-$  in the shallow groundwater are large, indicating strong spatial dispersion in the shallow groundwater and uneven distribution in the entire study area. However, the concentrations in human aggregation areas, such as Gaotai, and irrigated areas are relatively high. The analytical results suggest that shallow groundwater is sensitive to agricultural irrigation, industrial production, domestic sewage and other human activities, resulting in elevated concentrations of  $\text{K}^+$ ,  $\text{Cl}^-$  and  $\text{NO}_3^-$  in areas with intensive land use activities. The variation coefficients of  $\text{Na}^+$ ,  $\text{Ca}^{2+}$ ,  $\text{Mg}^{2+}$ ,  $\text{HCO}_3^-$ ,  $\text{SO}_4^{2-}$ ,  $\text{PO}_4^{3-}$  and Fe are small, indicating that these ions are relatively stable in the entire study area (Weber 2010).

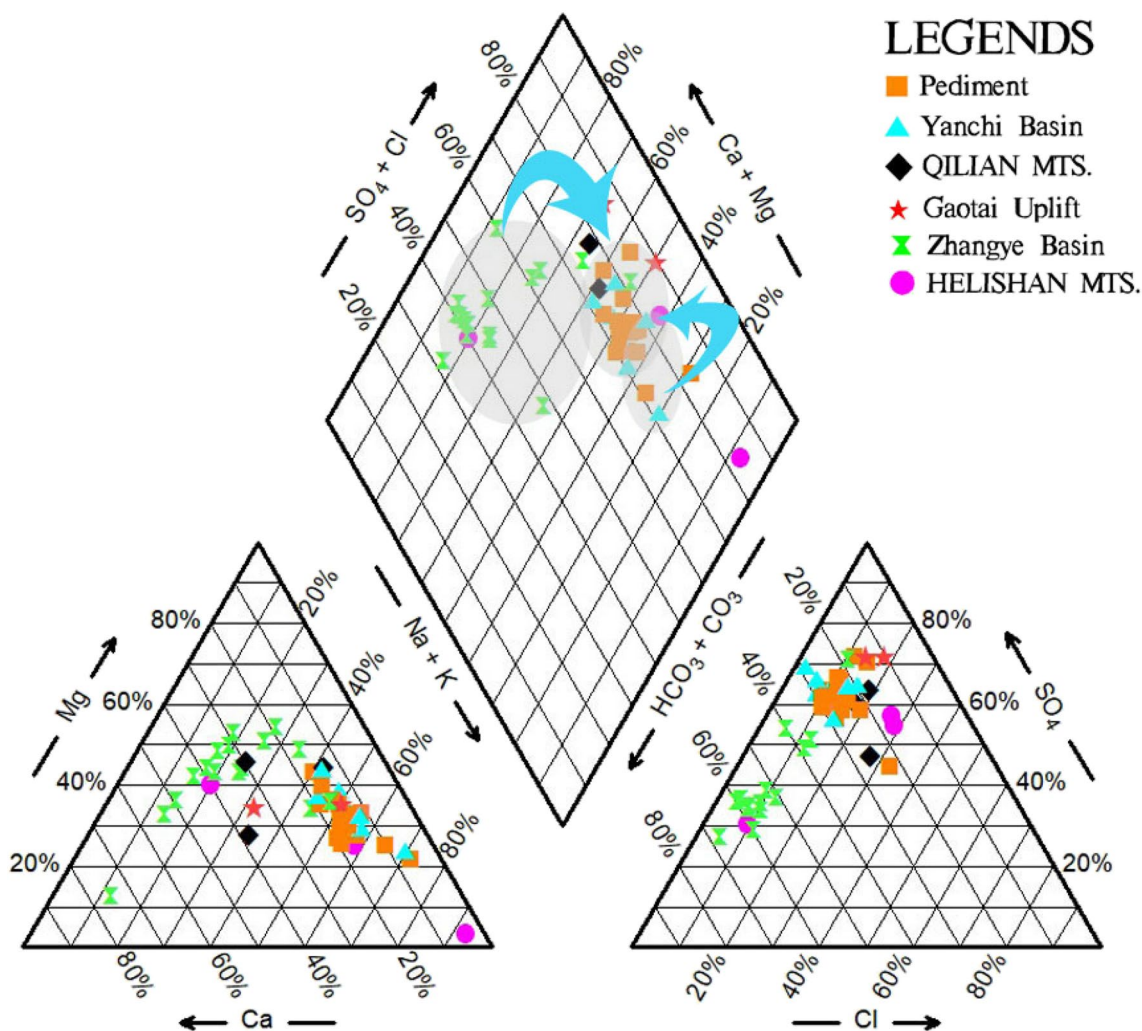


Fig. 5 Groundwater hydrochemistry types in the middle reaches of the Heihe River catchment

**Spatial variations in the chemical composition of groundwater**

A Piper diagram (Fig. 5) and a TDS contour map (Fig. 6) of the shallow groundwater in the study area indicate the following:

The TDS of the shallow groundwater in the Zhangye Basin gradually increased in the direction of groundwater flow from the Qilian Mountains to the Longshou Shan piedmont alluvial plain in the north, with an average value of 976 mg/L. Along the groundwater flow paths, the main cations changed from  $Ca^{2+}$  and  $Mg^{2+}$  to  $Na^{+}$ . The main anion in the groundwater was  $HCO_3^{-}$ , and the main chemical composition gradually changed in the direction of groundwater flow from  $HCO_3^{-}-SO_4^{2-}-Ca^{2+}-Mg^{2+}$  to  $HCO_3^{-}-SO_4^{2-}-Na^{+}-Mg^{2+}$ .

The TDS of shallow groundwater in the Qilian Mountains is approximately 2000 mg/L. The main groundwater

cation in this area is  $Na^{+}$ , the main anion is  $SO_4^{2-}$ , and the main hydrochemical type is  $SO_4^{2-}-HCO_3^{-}-Na^{+}-Mg^{+}$ . In contrast, the average TDS of the shallow groundwater in the Gaotai uplift is generally more than 2000 mg/L. The main cation in this area is  $Na^{+}$ , the main anion is  $SO_4^{2-}$ , and the main hydrochemical type is  $SO_4^{2-}-Na^{+}-Mg^{2+}$ .

The TDS of the shallow groundwater in the Heli Shan area gradually decreased from the mountain area to the foot of the mountain. In the Heli Shan area, the main cation is  $Na^{+}$ , the main anion is  $SO_4^{2-}$ , and the main hydrochemical type is  $SO_4^{2-}-Na^{+}$ . At the foot of Heli Shan, the main cations are  $Na^{+}$  and  $Ca^{2+}$ , the main anions are  $SO_4^{2-}$  and  $HCO_3^{-}$ , and the main hydrochemical types are  $SO_4^{2-}-Cl^{-}-Na^{+}-Mg^{2+}$  and  $HCO_3^{-}-SO_4^{2-}-Ca^{2+}-Mg^{2+}$ .

The TDS of the shallow groundwater in the Yanchi Basin increases from southwest to northeast, with an average value of 956 mg/L. The main cations in the groundwater in this area are  $Na^{+}$  and  $Mg^{2+}$ , and the

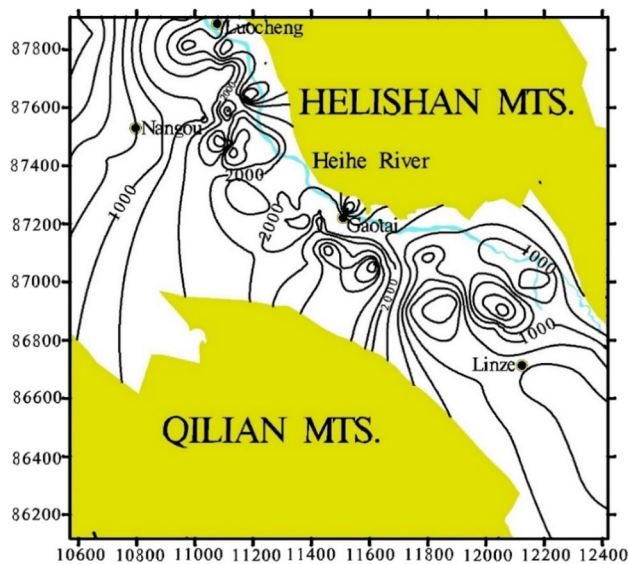


**Fig. 6** Main study area TDS contour map

**Table 1** Shallow groundwater chemical parameter statistical results

| Chemical parameters                  | Shallow groundwater |      |        |       |      |
|--------------------------------------|---------------------|------|--------|-------|------|
|                                      | Max                 | Min  | Mean   | StDev | CV   |
| pH                                   | 9.72                | 7.26 | 7.87   | 0.35  | 0.04 |
| TDS (mg/L)                           | 4507                | 205  | 1756   | 947   | 0.54 |
| Na <sup>+</sup> (mg/L)               | 1102                | 13   | 328    | 235   | 0.71 |
| K <sup>+</sup> (mg/L)                | 94                  | 2    | 12     | 13    | 1.1  |
| Ca <sup>2+</sup> (mg/L)              | 282                 | 20   | 95     | 51    | 0.54 |
| Mg <sup>2+</sup> (mg/L)              | 302.9               | 13.4 | 112.91 | 64.55 | 0.57 |
| HCO <sub>3</sub> <sup>-</sup> (mg/L) | 842                 | 85   | 385    | 159   | 0.41 |
| Cl <sup>-</sup> (mg/L)               | 1103                | 3.5  | 188    | 197   | 1.04 |
| F <sup>-</sup> (mg/L)                | 2.71                | 0.08 | 0.48   | 0.42  | 0.88 |
| NO <sub>3</sub> <sup>-</sup> (mg/L)  | 257.04              | 0    | 38     | 49    | 1.27 |
| SO <sub>4</sub> <sup>2-</sup> (mg/L) | 2181                | 46   | 782    | 457   | 0.59 |
| PO <sub>4</sub> <sup>3-</sup> (mg/L) | 0.06                | 0.02 | 0.03   | 0.01  | 0.42 |
| Fe (mg/L)                            | 0.29                | 0.04 | 0.08   | 0.07  | 0.89 |

main anion is SO<sub>4</sub><sup>2-</sup>. The main hydrochemical types are SO<sub>4</sub><sup>2-</sup>-HCO<sub>3</sub><sup>-</sup>-Na<sup>+</sup>-Mg<sup>2+</sup> and SO<sub>4</sub><sup>2-</sup>-HCO<sub>3</sub><sup>-</sup>-Mg<sup>2+</sup>-Na<sup>+</sup>. There are more alkali metal ions than alkaline earth metal ions in this region.

The average TDS of the shallow groundwater in the Pediment area is 1727 mg/L. The main cation is Na<sup>+</sup>, the main anion is SO<sub>4</sub><sup>2-</sup>, and the main hydrochemical type is SO<sub>4</sub><sup>2-</sup>-Na<sup>+</sup>-Mg<sup>2+</sup>.

Overall, the upper TDS of the groundwater flow from the recharge area to the discharge area gradually increases (Fig. 6). The chemical composition of groundwater changes from SO<sub>4</sub><sup>2-</sup>-HCO<sub>3</sub><sup>-</sup>-Na<sup>+</sup>-Mg<sup>2+</sup> in the Qilian Mountains to SO<sub>4</sub><sup>2-</sup>-HCO<sub>3</sub><sup>-</sup>-Na<sup>+</sup>-Mg<sup>2+</sup> and

from SO<sub>4</sub><sup>2-</sup>-HCO<sub>3</sub><sup>-</sup>-Mg<sup>2+</sup>-Na<sup>+</sup> in the Yanchi Basin to SO<sub>4</sub><sup>2-</sup>-Na<sup>+</sup>-Mg<sup>2+</sup> type in the Pediment area.

### Analysis of the hydrochemical origin of the shallow groundwater

Various factors control the hydrochemical evolution of groundwater. The dissolved components in groundwater and their correlations are effective means to reveal the likely sources of dissolved substances in the water and the hydrochemical processes that have given rise to the groundwater chemical composition and its salinity (Fisher and Iii 1997).

### Correlation analysis

Total soluble solids (TDSs) are a measure of the total amount of main ions that are present in groundwater (Zhou et al. 2007), and TDSs are an important index for studying the chemical characteristics of groundwater. A correlation matrix reveals that TDS is highly correlated with SO<sub>4</sub><sup>2-</sup>, Na<sup>+</sup> and Cl<sup>-</sup>. That is, SO<sub>4</sub><sup>2-</sup>, Na<sup>+</sup> and Cl<sup>-</sup> are the main influencing factors of TDS. According to the correlation matrix (Table 2), SO<sub>4</sub><sup>2-</sup>, Na<sup>+</sup> and Cl<sup>-</sup> also exhibit strong correlations with each other, which suggests that either these ions have a similar source or that their concentrations in groundwater are influenced by the same processes.

Most of the sampling sites are located in the Pediment, and most of the sites are located in the groundwater discharge area. Under natural conditions, the SO<sub>4</sub><sup>2-</sup>, Na<sup>+</sup> and Cl<sup>-</sup> in the study area likely originate in evaporite dissolution, which possibly contributes to the deposition of marine-derived salts in rainfall. The dissolution of soluble salts likely occurs in recharge areas such as the Qilian Mountains and Longshou Shan, and SO<sub>4</sub><sup>2-</sup>, Na<sup>+</sup> and Cl<sup>-</sup> progressively increases in the direction of groundwater flow due to continuing water-rock reactions and the effects of evaporation in areas where the water table is present at shallow depths.

### Cation exchange and adsorption

The extent to which cation exchange and adsorption occurs by mineral surfaces in an aquifer can be determined by the use of chloralkali indices (chloroalkaline indices) (Aghazadeh and Mogaddam 2010; Wang 2013). The two chloroalkaline indices, CAI-I and CAI-II, are calculated using the following formulas:

$$\text{CAI-I} = \frac{\text{Cl}^- - (\text{Na}^+ + \text{K}^+)}{\text{Cl}^-} \quad (1)$$

$$\text{CAI-II} = \frac{\text{Cl}^- - (\text{Na}^+ + \text{K}^+)}{\text{HCO}_3^- + \text{SO}_4^{2-} + \text{CO}_3^{2-} + \text{NO}_3^-} \quad (2)$$



**Table 2** Correlation matrices of ions in the shallow groundwater of the study area

| Ions                          | Na <sup>+</sup> | K <sup>+</sup> | Ca <sup>2+</sup> | Mg <sup>2+</sup> | HCO <sub>3</sub> <sup>-</sup> | Cl <sup>-</sup> | F <sup>-</sup> | NO <sub>3</sub> <sup>-</sup> | SO <sub>4</sub> <sup>2-</sup> | TDS     | pH       |
|-------------------------------|-----------------|----------------|------------------|------------------|-------------------------------|-----------------|----------------|------------------------------|-------------------------------|---------|----------|
| Na <sup>+</sup>               | 1               | 0.327**        | 0.305**          | 0.461**          | 0.180                         | 0.835**         | 0.613**        | 0.057                        | 0.883**                       | 0.917** | -0.085   |
| K <sup>+</sup>                |                 | 1              | 0.421**          | 0.579**          | 0.247*                        | 0.428**         | 0.079          | 0.057                        | 0.494**                       | 0.509** | -0.145   |
| Ca <sup>2+</sup>              |                 |                | 1                | 0.572**          | 0.335**                       | 0.454**         | 0.262*         | 0.425**                      | 0.526**                       | 0.570** | -0.364** |
| Mg <sup>2+</sup>              |                 |                |                  | 1                | 0.542**                       | 0.498**         | 0.121          | 0.411**                      | 0.748**                       | 0.750** | -0.359** |
| HCO <sub>3</sub> <sup>-</sup> |                 |                |                  |                  | 1                             | 0.020           | 0.088          | 0.404**                      | 0.298**                       | 0.353** | -0.378** |
| Cl <sup>-</sup>               |                 |                |                  |                  |                               | 1               | 0.548**        | 0.040                        | 0.718**                       | 0.828** | -0.104   |
| F <sup>-</sup>                |                 |                |                  |                  |                               |                 | 1              | 0.082                        | 0.443**                       | 0.514** | -0.069   |
| NO <sub>3</sub> <sup>-</sup>  |                 |                |                  |                  |                               |                 |                | 1                            | 0.211*                        | 0.265** | -0.087   |
| SO <sub>4</sub> <sup>2-</sup> |                 |                |                  |                  |                               |                 |                |                              | 1                             | 0.971** | -0.228*  |
| TDS                           |                 |                |                  |                  |                               |                 |                |                              |                               | 1       | -0.233*  |
| pH                            |                 |                |                  |                  |                               |                 |                |                              |                               |         | 1        |

\*Indicates a significant correlation at the level of 0.05

\*\*Indicates a significant correlation at the level of 0.01

Negative chloroalkaline indices signify that Ca<sup>2+</sup> and Mg<sup>2+</sup> in the water have exchanged for Na<sup>+</sup> and K<sup>+</sup> on mineral surfaces in the aquifer. If the indices are positive, the opposite exchange has occurred.

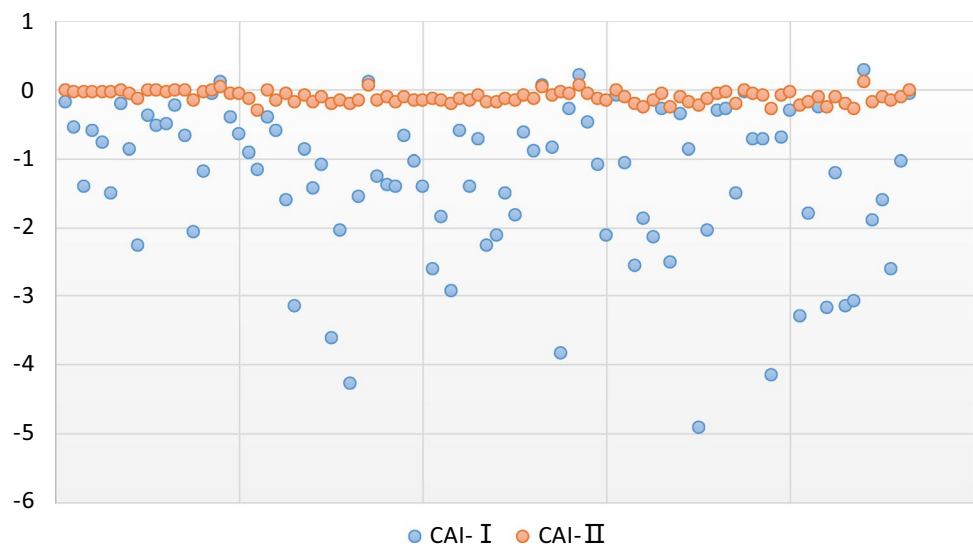
Calculations for the samples collected in this study indicated that the chloroalkaline index values for the majority of the samples are less than 0 (Fig. 7), which indicates that cation exchange and adsorption can occur within the study area. Therefore, from the recharge area to the discharge area, Ca<sup>2+</sup> and Mg<sup>2+</sup> in the groundwater displace Na<sup>+</sup> in the aquifer matrix along the groundwater flow path, which causes increases in the proportion and concentration of sodium ions in groundwater.

### Evaporative concentration of groundwater

The groundwater discharge from the shallow aquifer mainly occurs by evaporation, particularly under conditions of drought (Chen et al. 2006). The evaporation of groundwater and the retention of salt in the groundwater result in the continuous concentration of the groundwater solution and increase the concentration of SO<sub>4</sub><sup>2-</sup>, Na<sup>+</sup> and Cl<sup>-</sup>. Therefore, the groundwater in the discharge area of the Yanchi Basin is highly mineralized, and salinization often occurs on the surface.

In addition, according to the variation coefficient analysis of water chemical parameters, SO<sub>4</sub><sup>2-</sup> and Na<sup>+</sup> are uniformly distributed in the regional groundwater. However, Cl<sup>-</sup> is more unevenly distributed with locally high concentrations, which could indicate that there is human influence on the distribution of this anion in the groundwater. However, as

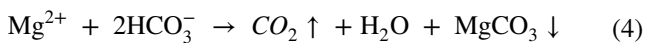
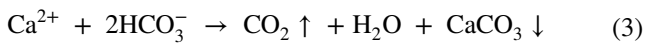
**Fig. 7** Water sample chloroalkaline index calculation results



most of the sampling points were located in non-urban parts of the groundwater discharge area, it is more likely that the  $\text{Cl}^-$  in the samples was primarily affected by natural factors. Concentrations of  $\text{SO}_4^{2-}$ ,  $\text{Na}^+$  and  $\text{Cl}^-$  are relatively high in the groundwater throughout the groundwater discharge area and possibly have the same source.

### Decarbonation

The groundwater pH is negatively correlated with  $\text{Ca}^{2+}$ ,  $\text{Mg}^{2+}$ , and  $\text{HCO}_3^-$ , and the correlation coefficients of the three are similar. That is,  $\text{Ca}^{2+}$ ,  $\text{Mg}^{2+}$ , and  $\text{HCO}_3^-$  have basically the same influence on pH. In the discharge area, the groundwater flows upward, the vertical pressure of the groundwater decreases, and the temperature increases. The partially dissolved  $\text{CO}_2$  in the groundwater is converted into a free state, and decarbonation occurs:



Decarbonation results in the precipitation of  $\text{CaCO}_3$  and  $\text{MgCO}_3$  (Ma et al. 2012), decreased  $\text{HCO}_3^-$ ,  $\text{Ca}^{2+}$  and  $\text{Mg}^{2+}$  in the groundwater, and decreased TDS. In addition, the

dominant cation converts to  $\text{Na}^+$ . Therefore, the percentage of  $\text{HCO}_3^-$  mg-equivalent decreases from 30~40 to 20~30 along the groundwater flow path from the Qilian Mountains to the pediment.

### Mixing of groundwater from different sources

The saturation index (SI) can indicate the dissolution status of minerals (Prasanna et al. 2010). The specific SI expression is as follows:

$$\text{SI} = \lg \frac{\text{IAP}}{K} \quad (5)$$

where IAP is the ion activity product, and K is an equilibrium constant. When  $\text{SI}=0$ , the minerals in the solution reach an equilibrium state. When  $\text{SI}<0$ , the minerals in the solution are unsaturated and continue to dissolve. When  $\text{SI}>0$ , the minerals in the solution are oversaturated, and precipitates are formed.

According to the groundwater flow direction, two flow paths were selected, (Line 1 and Line 2, respectively; Fig. 8), and the saturation index of the main minerals in the shallow groundwater was simulated along each of these flow paths.

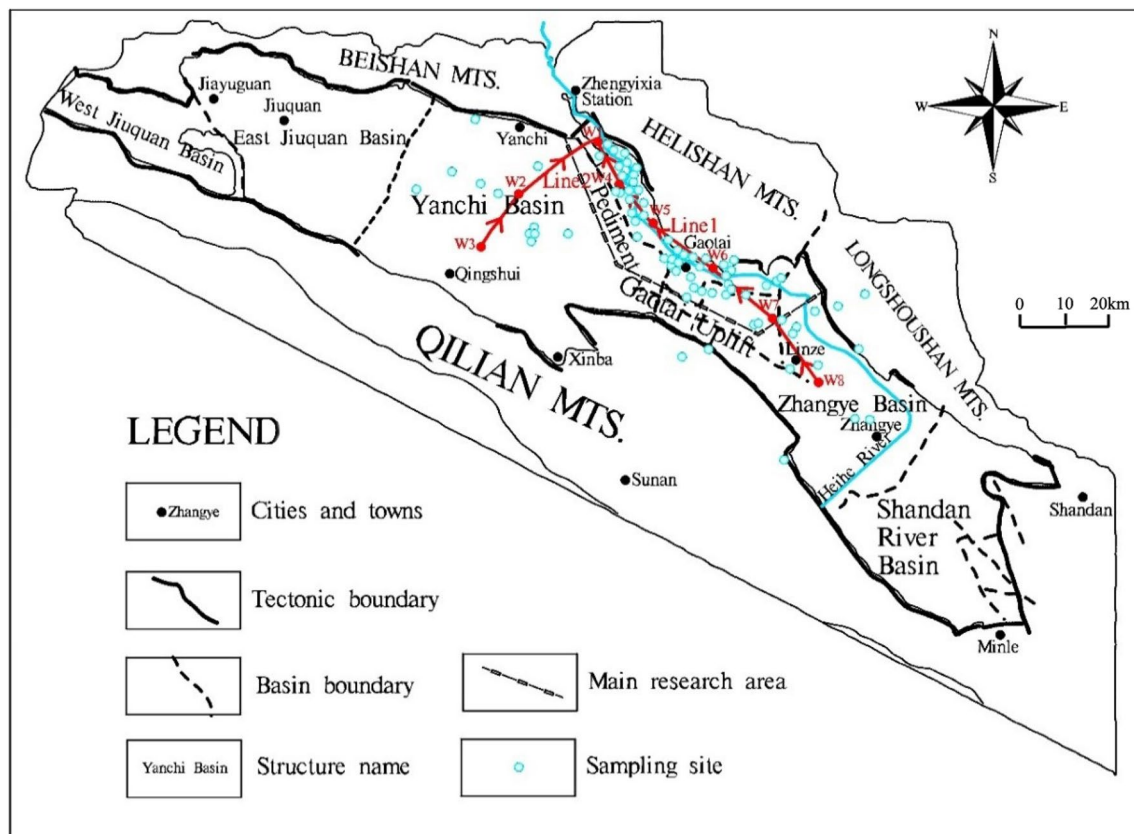


**Fig. 8** Saturation index simulation point locations and flow paths

As shown in Table 3, the saturation index of gypsum, carbon dioxide gas, anhydrite and halite is always less than 0, indicating that groundwater does not become saturated with respect to these constituents along each flow path. In addition, the saturation indices of aragonite, calcite and dolomite are always greater than 1, indicating that groundwater along each flow path is saturated with respect to these mineral phases, and these minerals are likely to be precipitating from solution within the aquifer.

The saturation index values of aragonite, calcite and dolomite first increased along Line 1, then decreased at W1 and W4, decreased along Line 2 and finally increased at W1 and W4. The analytical results indicate that the groundwater flow mixes in the Pediment, where W1 and W4 are located, which causes water with two different chemical compositions to mix, thus making the mineral saturation index values of the groundwater from the two sources close to the mean value. This outcome is also supported by the Piper diagram plot of the groundwater data from the area.

**Assessment of ion ratios**

$\gamma(\text{HCO}_3^- + \text{SO}_4^{2-})/\gamma(\text{Ca}^{2+} + \text{Mg}^{2+})$  As shown in Fig. 9, most of the water sample points in the Zhangye Basin are distributed along the line  $\gamma(\text{HCO}_3^- + \text{SO}_4^{2-})/\gamma(\text{Ca}^{2+} + \text{Mg}^{2+}) = 1:1$ , indicating that the  $\text{HCO}_3^-$ ,  $\text{SO}_4^{2-}$ ,  $\text{Ca}^{2+}$  and  $\text{Mg}^{2+}$  in the groundwater of this area primarily originate from the dissolution of sulphate minerals (gypsum) and carbonate minerals (calcite and dolomite). In contrast, most of the points in other areas are below the line, indicating that their  $\text{Ca}^{2+}$  and  $\text{Mg}^{2+}$  have other sources.

$\gamma\text{Cl}^-/\gamma\text{Na}^+$  A plot of the ratio of Cl/Na versus chloride concentration indicates that the groundwater sampling points are mainly below the 1:1 line (Fig. 10), indicating that cation exchange processes have some influence on the concentration of  $\text{Na}^+$  in solution.

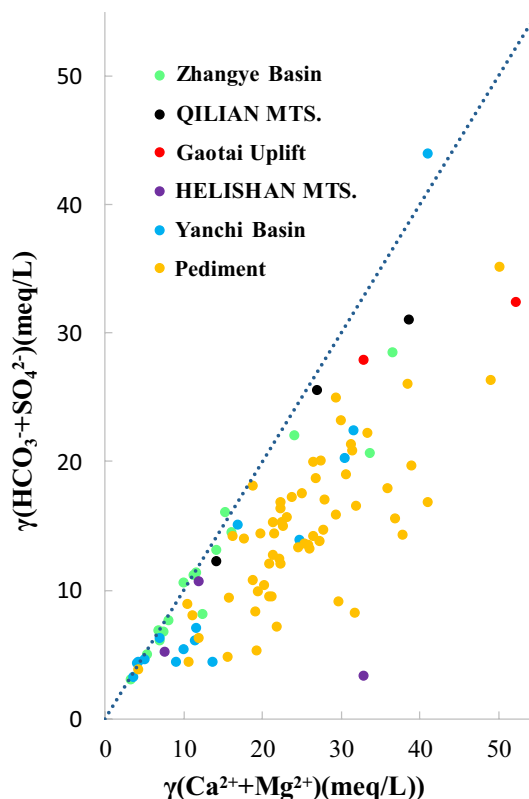


**Fig. 9** Plot of  $(\text{HCO}_3^- + \text{SO}_4^{2-})$  against  $(\text{Ca}^{2+} + \text{Mg}^{2+})$  in concentration units of meq/L

The  $\text{Na}^+$  content in the groundwater sample from the Yanchi Basin is significantly higher than in other samples because of its location in a groundwater discharge area where intensive evaporative concentration occurs.

**Gibbs diagram**

A plot of the groundwater data on a Gibbs diagram (Fig. 11) indicates that most of the Zhangye Basin samples plot in

**Table 3** Mineral and gas saturation index values for each sampling point

| Sample | Location      | Well depth (m) | Anhydrite (CaSO <sub>4</sub> ) | Aragonite (CaCO <sub>3</sub> ) | Calcite (CaCO <sub>3</sub> ) | CO <sub>2</sub> (g) | Dolomite [Ca·Mg(CO <sub>3</sub> ) <sub>2</sub> ] | Gypsum (CaSO <sub>4</sub> ·2H <sub>2</sub> O) | Halite (NaCl) |
|--------|---------------|----------------|--------------------------------|--------------------------------|------------------------------|---------------------|--|---|---------------|
| W1     | Pediment      | 39             | -1.37                          | 0.67                           | 0.81                         | -2.23               | 2.25   | -1.15   | -6.07         |
| W2     | Yanchi Basin  | 17.14          | -2.32                          | 0.12                           | 0.27                         | -2.85               | 1.04   | -2.1  | -7.48         |
| W3     | Yanchi Basin  | 50             | -2.41                          | 0.45                           | 0.59                         | -3.3                | 1.75   | -2.19   | -7.76         |
| W4     | Pediment      | 50             | -1.36                          | 0.41                           | 0.56                         | -2.17               | 1.57   | -1.14   | -5.49         |
| W5     | Pediment      | 13.43          | -1.26                          | 0.95                           | 1.09                         | -2.41               | 2.75   | -1.04   | -6.01         |
| W6     | Pediment      | 17.1           | -1.11                          | 0.8                            | 0.94                         | -2.32               | 2.15   | -0.89   | -6            |
| W7     | Zhangye Basin | 20             | -2.56                          | 0.75                           | 0.9                          | -3.61               | 2.09   | -2.34   | -8.63         |
| W8     | Zhangye Basin | 47             | -1.52                          | 0.62                           | 0.76                         | -1.95               | 1.44   | -1.3  | -7.6          |

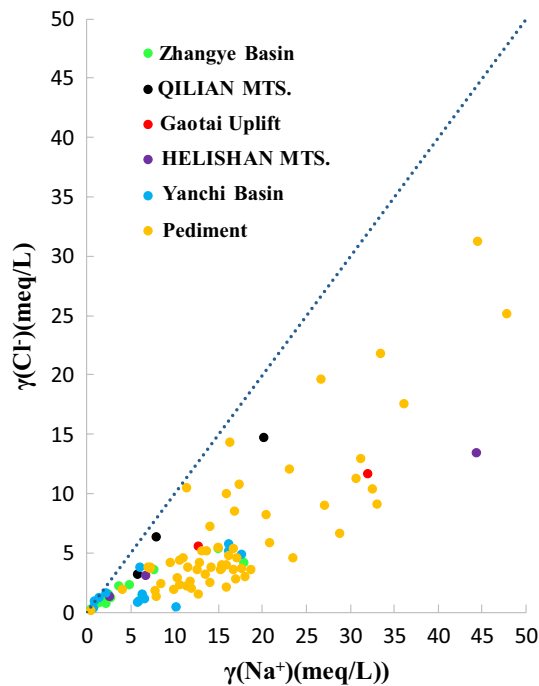


Fig. 10 A plot of Na<sup>+</sup> versus the concentration of Cl<sup>-</sup> in groundwater

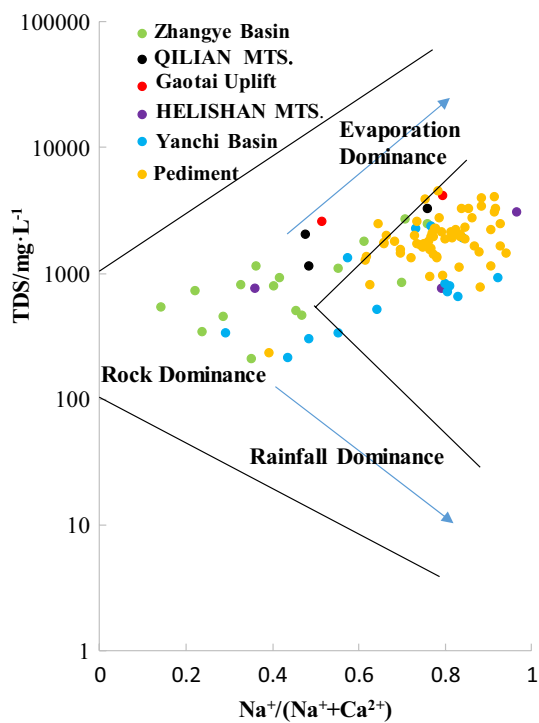


Fig. 11 Use of a Gibbs diagram to assess influences on groundwater quality

the rock weathering field on the diagram and that only a small number of samples plot in the evaporation field. This finding suggests that the chemical composition of the

shallow groundwater in the Zhangye Basin is affected by both weathering and evaporative concentration processes, although weathering appears to have a dominant influence on the groundwater composition in this area.

The Gibbs diagram indicates that the chemical composition of groundwater from the Qilian Mountains, Heli Shan and the Gaotai uplift areas are similar and are primarily affected by evaporation and crystallization of soluble salts. Several groundwater samples from these areas plot outside of the Gibbs diagram fields, suggesting that their chemical composition may have been partially influenced by the effects of human activities.

Most of the groundwater samples from the Yanchi Basin plot in the rock weathering and evaporation fields on the Gibbs diagram, indicating that the chemical composition of the shallow groundwater in this area is affected by both weathering and evaporative crystallization, and both of these factors have a similar level of influence on groundwater quality.

Most of the groundwater samples from the Pediment area plot in the evaporation field on the Gibbs diagram, although some samples from this area also plot outside of the Gibbs diagram fields, suggesting that human activity in this area also has an influence on the chemical composition of groundwater. However, due to the intense effect of evaporation on the TDS of groundwater in this area, we believe the pediment shallow groundwater chemical composition is primarily controlled by evaporation and crystallization of soluble salts, and the influence of human land use on TDS is likely to be small.

In the Gibbs' diagram, the shallow groundwater samples in the study area are not distributed in the rainfall dominant zone. That is, the atmospheric precipitation is probably not the main source of the shallow groundwater in this region. To verify this conclusion, the hydrogen and oxygen isotopes of the shallow groundwater in the study area were analysed, and the assessment results of these data are indicated below.

### Analysis of hydrogen and oxygen isotopes

Thirty-nine water samples were tested for hydrogen and oxygen isotopes, including 7 samples from the Yanchi Basin, 3 samples from the Qilian Mountains and 29 samples from the Pediment. A plot of  $\delta^{18}\text{O}$  and  $\delta^2\text{H}$  values for these samples is shown in Fig. 12.

Groundwater recharge sources can also be characterized by the deuterium surplus,  $d$ . In 1964, Dansgaard first proposed the concept of a deuterium surplus,  $d$ , which is numerically equal to the intercept when the slope of the precipitation line in a certain region is 8:

$$d = \delta^2\text{H} - 8 \times \delta^{18}\text{O} \tag{6}$$

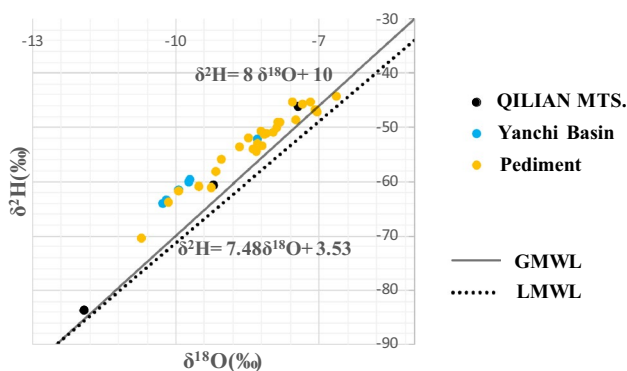


Fig. 12 Plot of  $\delta^{18}\text{O}$  versus  $\delta^2\text{H}$  for groundwater in the study area

The size of  $d$  is related to the precipitation temperature, air humidity and the dynamic fractionation coefficient of  $\delta^{18}\text{O}$  and  $\delta^2\text{H}$  in the falling water vapour. The deuterium surplus of each region in the study area is as follows (Table 4).

Normally,  $\delta^{18}\text{O}-\delta^2\text{H}$  will change in the circulation process of atmospheric precipitation and groundwater flow such that  $\delta^{18}\text{O}-\delta^2\text{H}$  will fall below the local precipitation line. Clark and Fritz (1997) indicated that a  $\delta^{18}\text{O}-\delta^2\text{H}$  ratio of a water sample that falls above the local precipitation line rarely occurs and indicates that there is either a deuterium excess or a  $\delta^{18}\text{O}$  deficiency. Certain scholars believe that the precipitation above the local precipitation line is affected by the ice melt water supply (Osterberg et al. 2006).

Our results reveal that the  $\delta^{18}\text{O}-\delta^2\text{H}$  ratios of the samples all fall above and to the left of the local precipitation line. The  $\delta^{18}\text{O}$ ,  $\delta^2\text{H}$  and  $d$  values in the Qilian Mountains, the Yanchi Basin and the Pediment indicate  $\delta^{18}\text{O}$  values from  $-10.26$  to  $-7.04\text{‰}$ ,  $\delta^2\text{H}$  values from  $-63.96$  to  $-47.18\text{‰}$ , and  $d$  values from  $9.14$ – $18.18\text{‰}$ , respectively. These results are very similar to those found in previous studies in this area. In addition, the  $\delta^{18}\text{O}-\delta^2\text{H}$  values of groundwater samples from the Yanchi Basin plot far from the local precipitation line, suggesting that the shallow groundwater supply source of the basin is mainly derived from ice and snow melt water from the Qilian Mountains.

This outcome is consistent with the conclusion obtained from the Gibbs diagram that the Yanchi Basin hydrochemistry is only marginally affected by rainfall. The Pediment  $\delta^{18}\text{O}$  value ranges from  $-10.7$  to  $-6.63\text{‰}$ , the  $\delta^2\text{H}$

value is from  $-70.55$  to  $44.35\text{‰}$ , and the  $d$  value is from  $8.69$ – $17.74\text{‰}$ . Thus, the replenishment sources of the Pediment are complex. The preceding results reveal that half of the points are distributed near the global precipitation line, while the other half are far from the precipitation line, indicating that the region is replenished by both atmospheric precipitation and snowmelt. The  $\delta^{18}\text{O}$  value of the Qilian Mountains ranges from  $-11.92$  to  $-7.43\text{‰}$ , the  $\delta^2\text{H}$  is from  $-83.82$  to  $-46.14\text{‰}$ , and the  $d$  value is from  $11.54$ – $13.3\text{‰}$ . Combining these outcomes with the previous analysis, the main source of groundwater recharge in the Qilian Mountains is seepage from the beds of rivers (primarily the Heihe River and Liyuan River), which originate from the Qilian Mountains.

### Conclusion

Groundwater in the middle reaches of the Heihe River occurs in a regionally extensive groundwater flow system. Most of the shallow groundwater in the study area is brackish and weakly alkaline. The main anions in the groundwater are  $\text{SO}_4^{2-}$  and  $\text{Na}^+$ . Concentrations of  $\text{SO}_4^{2-}$ ,  $\text{NO}_3^-$ ,  $\text{Cl}^-$  and  $\text{Na}^+$  in groundwater greatly exceed those of  $\text{F}$  and  $\text{Fe}$ , and all of the ions are of natural origin. The variation coefficient ( $C_v$ ) of  $\text{K}^+$ ,  $\text{Cl}^-$  and  $\text{NO}_3^-$  in the shallow groundwater is large, and these ions are unevenly distributed throughout the entire region, while other ions are relatively evenly distributed in the groundwater.

TDS increases gradually in the groundwater flow direction from the recharge area to the discharge area in the study area. The groundwater chemical type is transformed from  $\text{SO}_4^{2-}-\text{HCO}_3^- -\text{Na}^+-\text{Mg}^{2+}$  in the Qilian Mountains to  $\text{SO}_4^{2-}-\text{HCO}_3^- -\text{Mg}^{2+}-\text{Na}^+$  and  $\text{SO}_4^{2-}-\text{HCO}_3^- -\text{Na}^+-\text{Mg}^{2+}$  in the salt basins to  $\text{SO}_4^{2-}-\text{Na}^+-\text{Mg}^{2+}$  in the Pediment. From the Qilian Mountains to Longshou Shan, the groundwater chemical composition in the Zhangye Basin gradually changes from  $\text{HCO}_3^- -\text{SO}_4^{2-}-\text{Ca}^{2+}-\text{Mg}^{2+}$  to  $\text{HCO}_3^- -\text{SO}_4^{2-}-\text{Na}^+-\text{Mg}^{2+}$ . The groundwater chemical composition in both the Zhangye Basin and the Yanchi Basin gradually changes as the water flows to the Pediment. Based on the groundwater flow analysis, the water flows of the Zhangye Basin and of the Yanchi Basin converge at the Pediment, resulting in a mixing effect,

Table 4 Study area  $\delta^{18}\text{O}$ ,  $\delta^2\text{H}$  and  $d$  statistics

| Parameter    | $\delta^{18}\text{O}$ |        |       |      | $\delta^2\text{H}$ |        |        |       | $d$   |       |       |      |
|--------------|-----------------------|--------|-------|------|--------------------|--------|--------|-------|-------|-------|-------|------|
|              | Max                   | Min    | Mean  | SD   | Max                | Min    | Mean   | StDev | Max   | Min   | Mean  | SD   |
| Pediment     | -6.63                 | -10.7  | -8.29 | 1.00 | -44.35             | -70.55 | -53.04 | 6.45  | 17.74 | 8.69  | 13.31 | 2.29 |
| Yanchi Basin | -7.04                 | -10.26 | -9.30 | 1.20 | -47.18             | -63.96 | -58.28 | 6.24  | 18.18 | 9.14  | 16.16 | 3.42 |
| Qilian MTS.  | -7.43                 | -11.92 | -9.52 | 2.26 | -46.14             | -83.82 | -63.54 | 19.00 | 13.3  | 11.54 | 12.59 | 0.93 |

which influences the groundwater chemical composition in the discharge area.

The groundwater chemical composition varies greatly throughout the study area. The ionic concentrations of  $\text{SO}_4^{2-}$ ,  $\text{Na}^+$  and  $\text{Cl}^-$  comprise most of the groundwater TDS content. These ions are mainly derived from the dissolution of soluble salts by groundwater flow, and their concentrations are increased in the discharge area by the effects of evaporation.

The calculation of chloroalkaline indices suggests that cation exchange and adsorption occur across the entire study area. Groundwater pH displays a significant negative correlation with  $\text{Ca}^{2+}$ ,  $\text{Mg}^{2+}$  and  $\text{HCO}_3^-$ , which is primarily due to the effect of decarbonation in the study area. Saturation index calculations indicate that groundwater from different sources mixes in the Pediment area and changes the chemical composition of the resultant groundwater.

The assessment of the groundwater data with a Gibbs diagram indicates that the chemical composition of the study area is primarily affected by rock weathering, evaporation, and crystallization of soluble salts.

Additionally, the groundwater chemical composition suggests that precipitation is not a major source of recharge for the shallow aquifer. The  $\delta^{18}\text{O}$ ,  $\delta^2\text{H}$  and  $d$  results suggest that shallow groundwater recharge in the Yanchi Basin is primarily derived from ice and snow meltwater from the Qilian Mountains, and the Pediment is simultaneously replenished by precipitation and ice and snow meltwater. The main source of recharge in the Qilian Mountains is riverbed seepage, which is mainly from the Heihe River and the Liyuan River.

**Acknowledgements** This work was supported by Center for Hydrogeology and Environmental Geology Survey, *China Geological Survey*. Funded projects are “A 1:50,000 hydrogeological survey of the Heihe river basin in the hexi corridor (DD20160292)” and “Major research project of the national natural science foundation of China: observation and mechanism research on the mutual transformation of surface water and groundwater in Heihe river basin (91025019)”.

## References

- Aghazadeh N, Mogaddam AA (2010) Assessment of groundwater quality and its suitability for drinking and agricultural uses in the Oshnavieh area, Northwest of Iran. *J Environ Prot* 1:30–40
- Bouragba L, Mudry J, Bouchaou L, Hsissou Y, Krimissa M, Tagma T, Michelot J (2011) Isotopes and groundwater management strategies under semi-arid area: case of the Souss upstream basin (Morocco). *Appl Radiat Isot* 69:1084–1093
- Chen R, Kang E, Ji X, Yang J, Zhang Z, Yang Y (2006) Temporal variations of  $\text{CO}_2$  concentration near land surface and its response to meteorological variables in Heihe River Basin, northwest China. *J Environ Sci (China)* 18:708–715
- Chen Y, Zhi LI, Fan Y, Wang H, Fang G (2014) Research progress on the impact of climate change on water resources in the arid region of Northwest China. *Acta Geogr Sin* 69:1295–1304
- Clark ID, Fritz P (1997) *Environmental isotopes in hydrogeology*. Lewis, Boca Raton
- Craig H (1961) *Isotopic Variations in Meteoric Waters Science* 133:1702–1703
- Dansgaard W (1964) Stable isotopes in precipitation *Tellus* 16:436–468
- Dong D-L et al (2007) Environmental characteristics of groundwater: an application of PCA to water chemistry analysis in Yulin. *J China Univ Min Technol* 17:73–77
- Fantong WY, Satake H, Ayonghe SN, Aka FT, Asai K (2009) Hydrogeochemical controls and usability of groundwater in the semi-arid Mayo Tsanaga River Basin: far north province, Cameroon. *Environ Geol* 58:1281–1293
- Feng Q, Liu W, Su YH, Zhang YW, Si JH (2004) Distribution and evolution of water chemistry in Heihe River basin. *Environ Geol* 45:947–956
- Fisher RS, Mullican WF III (1997) Hydrochemical evolution of sodium-sulfate and sodium-chloride groundwater beneath the northern Chihuahuan Desert, Trans-Pecos, Texas, USA. *Hydrogeol J* 5:4–16
- Gibbs RJ (1970) Mechanisms controlling world water chemistry. *Science* 170:1088–1090
- Gleick PH (2000) A look at twenty-first century water resources development. *Water Int* 25:127–138
- Huang C, Zheng C (2009) Spatial differentiation of water resources supply and demand balance in Fujian Province. *Resour Sci* 31:750–756
- Joshi A, Seth G (2011) Hydrochemical investigations and correlation analysis of groundwater quality. *J Environ Sci Eng* 53:151
- Liu H (2012) Comprehensive carrying capacity of the urban agglomeration in the Yangtze River Delta, China. *Habitat Int* 36:462–470
- Lu L, Cheng G, Li X (2001a) Landscape change in middle Heihe River Basin. *Chin J Appl Ecol* 12:68–74
- Lu L, Li X, Chen G, Xiao H (2001b) Analysis on the landscape structure of the Heihe River Basin, Northwest China. *Acta Ecol Sin* 21:1217–1224
- Ma Z, Dou H, Li T, Hu W, Yan H (2012) Geochemical study of groundwater mineralization in Guanzhong Basin, Shaanxi province, NW China. *Desalination and Water Treat* 42:317–322
- Ning BY, Yuan-Qing HE, Xian-Zhong HE, Zong-Xing LI (2008) Advances on water resources research in Heihe River Basin. *J Desert Res* 28:1180–1185
- Osterberg EC, Handley MJ, Sneed SB, Mayewski PA, Kreutz KJ (2006) Continuous ice core melter system with discrete sampling for major ion, trace element and stable isotope analyses. *Environ Sci Technol* 40:3355–3361
- Piper AM (1944) A graphic procedure in the geochemical interpretation of water-analyses. *Eos Trans Am Geophys Union* 25:914–928
- Prasanna MV, Chidambaram S, Hameed AS, Srinivasamoorthy K (2010) Study of evaluation of groundwater in Gadilam basin using hydrogeochemical and isotope data. *Environ Monit Assess* 168:63–90
- Qi SZ, Luo F (2005) Water environmental degradation of the Heihe River Basin in arid northwestern China. *Environ Monit Assess* 108:205
- Shen Y, Chen Y (2010) Global perspective on hydrology, water balance, and water resources management in arid basins. *Hydrol Process* 24:129–135
- Wang S (2013) Groundwater quality and its suitability for drinking and agricultural use in the Yanqi Basin of Xinjiang Province, Northwest China. *Environ Monit Assess* 185:7469
- Wang SW, Liu CW, Jang CS (2007) Factors responsible for high arsenic concentrations in two groundwater catchments in Taiwan. *Appl Geochem* 22:460–476
- Weber VL (2010) Coefficient of variation of underwater irradiance fluctuations. *Radiophys Quantum Electron* 53:13–27

- Yang X (2006) Chemistry and late Quaternary evolution of ground and surface waters in the area of Yabulai Mountains, western Inner Mongolia, China. *Catena* 66:135–144
- Zhou X, Zhang H, Zhao L, Ye S, Xia Y, Li R, Li Z (2007) Some factors affecting TDS and pH values in groundwater of the Beihai coastal area in southern Guangxi, China. *Environ Geol* 53:317–323

**Publisher's Note** Springer Nature remains neutral with regard to jurisdictional claims in published maps and institutional affiliations.